




Article

Synthesis of New Zirconium Magnetic Nanocomposite as a Bioactive Agent and Green Catalyst in the Four-Component Synthesis of a Novel Multi-Ring Compound Containing Pyrazole Derivatives

Mohammed Asiri ¹, **Ahmed Ghalib Abdulsalam** ², Mustafa Kahtan ³, Fahad Alsaikhan ⁴ , Issa Farhan ⁵, Dhameer A. Mutlak ⁶, Salema K. Hadrawi ⁷, Muath Suliman ¹, Ritamaria Di Lorenzo ^{8,*}  and Sonia Laneri ^{8,*} 

¹ Department of Clinical Laboratory Sciences, College of Applied Medical Sciences, King Khalid University, Abha 61421, Saudi Arabia

² Department of Pharmacy, Al-Noor University College, Bartella 46476, Iraq

³ Medical Technical College, Al-Farahidi University, Baghdad 10011, Iraq

⁴ College of Pharmacy, Prince Sattam Bin Abdulaziz University, Alkharj 11942, Saudi Arabia

⁵ Medical Physics Department, Al-Mustaqbal University College, Babylon 51001, Iraq

⁶ AL-Nisour University College, Baghdad 10001, Iraq

⁷ Refrigeration and Air-Conditioning Technical Engineering Department, College of Technical Engineering, The Islamic University, Najaf 54001, Iraq

⁸ Department of Pharmacy, School of Medicine and Surgery, University of Naples Federico II, Via D. Montesano, 49-80131 Naples, Italy

* Correspondence: ritamaria.dilorenzo@unina.it (R.D.L.); slaneri@unina.it (S.L.)



Citation: Asiri, M.; Abdulsalam, A.G.; Kahtan, M.; Alsaikhan, F.; Farhan, I.; Mutlak, D.A.; Hadrawi, S.K.; Suliman, M.; Di Lorenzo, R.; Laneri, S. Synthesis of New Zirconium Magnetic Nanocomposite as a Bioactive Agent and Green Catalyst in the Four-Component Synthesis of a Novel Multi-Ring Compound Containing Pyrazole Derivatives. *Nanomaterials* **2022**, *12*, 4468. <https://doi.org/10.3390/nano12244468>

Academic Editors: Alexey Pestryakov and Antonino Gulino

Received: 29 November 2022

Accepted: 11 December 2022

Published: 16 December 2022

Publisher's Note: MDPI stays neutral with regard to jurisdictional claims in published maps and institutional affiliations.



Copyright: © 2022 by the authors. Licensee MDPI, Basel, Switzerland. This article is an open access article distributed under the terms and conditions of the Creative Commons Attribution (CC BY) license (<https://creativecommons.org/licenses/by/4.0/>).

Abstract: New nanocomposites containing zirconium were synthesized using microwave irradiation. Their structure was confirmed by vibrating sample magnetometer (VSM) curves, X-ray diffraction (XRD) patterns, scanning electron microscope (SEM) and transmission electron microscopy (TEM) images, Fourier transform infrared spectroscopy (FT-IR), and Brunauer–Emmett–Teller (BET) N₂ adsorption/desorption isotherms. After the structure confirmation of the zirconium magnetic nanocomposite, the catalytic properties in the synthesis of pyrazole derivatives were investigated. Next, the biological activities of the zirconium magnetic nanocomposite, such as the antibacterial and antifungal activities, were investigated. The research results showed that the zirconium magnetic nanocomposite has high catalytic properties and can be used as a magnetic nanocatalyst for synthesizing heterocyclic compounds such as pyrazole derivatives in addition to having high biological properties. The unique properties of the nanoparticles can be attributed to their synthesis method and microwave radiation.

Keywords: zirconium magnetic nanocomposite; bioactive agent; green catalyst; four-component reaction; pyrazole derivatives; antibacterial activity; antifungal activity

1. Introduction

Cyclic organic compounds with at least one heteroatom, such as nitrogen, sulfur, and phosphorus, are called heterocycles. Heterocycles have many biological properties. There are heterocyclic compounds in the structures of many drugs. So far, biological properties such as antibacterial, antifungal, anticancer, and antioxidant properties of heterocyclic compounds containing nitrogen, sulfur, and phosphorus have been reported [1–7]. One of critical heterocyclic compounds' critical applications is their use as ligands in complexes. The use of heterocycles as ligands makes the final product retain the biological properties of the heterocycle and the metal, thus having high biological properties. There have been reports of using heterocycles as ligands and synthesizing novel complexes containing various metals such as Cr, Mo, W, gold, and silver. These have unique properties, including anticancer properties [8–12].

The heterocyclic compound of pyrazole with two nitrogen atoms in its structure has many biological properties. This heterocyclic ring is found abundantly in nature, and its valuable derivatives with biological properties have been extracted from natural compounds [13]. Biological properties, such as anticancer [14,15], anti-diabetic [16], antimicrobial [17,18], and antioxidant [19] of heterocyclic compounds containing pyrazole, have been reported. Considering their importance, it is necessary to provide new methods for its synthesis.

Recently, developments in green chemistry and multi-component reactions (MCRs) in synthesizing heterocyclic compounds, particularly for drugs, have increased dramatically. The factors driving this increase include the prevention of environmental pollution, economic efficiency, and high efficiency [20,21]. Another advantage of MCRs is that they perform the reaction in one step, reducing the products' synthesis time. In multi-component reactions, choosing a suitable catalyst is very important, and recently, nanocatalysts have proven to be effective in these reactions. Nanocatalysts have the added benefit of being recyclable and compatible with green chemistry. [22]. There have been several reports of various nanocatalysts, including metal oxide nanoparticles [23–25], magnetic nanoparticles [2,26], supported nanoparticles [27], and metal-organic framework nanoparticles [28], in the synthesis of organic and heterocyclic compounds.

Metal-organic framework nanoparticles are compounds with unique capabilities. High specific surface area and porosity are the main capabilities of these nanostructures, which have resulted in their application as flexible supercapacitors [29] and electrochemical biosensors for biomedical analysis [30,31]. There have been reports of these compounds being efficient and recyclable catalysts in synthesizing organic and heterocyclic compounds [32,33].

This study synthesized a new zirconium magnetic nanocomposite using Fe_3O_4 nanoparticles, dipicolinic acid, ZrCl_4 , and a microwave-assisted method. The final product's structure was identified and confirmed using VSM, XRD, SEM and TEM images, FT-IR, and BET. The final product was used as a catalyst candidate to synthesize new pyrazole derivatives and antimicrobial agents.

2. Materials and Methods

2.1. Solvents and Raw Materials

The high-purity solvents and raw materials used in this study were purchased from Merck and Sigma-Aldrich. The Fe_3O_4 nanostructures were prepared from Sigma-Aldrich. No purification of the raw materials was carried out (Merck KGaA, St. Louis, MO, USA).

2.2. Zirconium Magnetic Nanocomposite Synthesis

For the zirconium magnetic nanocomposite synthesis, Fe_3O_4 nanoparticles (2 mmol), dipicolinic acid (4 mmol), and ZrCl_4 (2 mmol) were added to 30 mL double-distilled water and stirred at 80 °C. After 10 min, the solution was put into a microwave and irradiated at a microwave power of 450 W at room temperature. After 10 min, the mixture cooled (room temperature), and the desired product was isolated using an external magnet. The synthesized zirconium magnetic nanocomposite was washed several times with a mix of double-distilled water and ethanol and dried at an ambient temperature.

2.3. Synthesis of 1,4-Dihydropyran[2,3-c]pyrazole-5-Carbonitrile Derivatives Using Zirconium Magnetic Nanocomposite as a Catalyst

For the synthesis of 1,4-dihydropyran[2,3-c]pyrazole-5-carbonitrile derivatives, zirconium magnetic nanocomposite (4 mg), aromatic aldehydes (1 mmol), and malononitrile (1 mmol) were added to 2 mL EtOH:H₂O and stirred at 50 °C for 5 min. Then, phenylhydrazine (1 mmol) and ethyl acetoacetate (1 mmol) was added and stirred at 50 °C. The reaction was monitored by thin-layer chromatography. After the completion of the reaction, the zirconium magnetic nanocomposite was separated using an external magnet. The synthesized 1,4-dihydropyran[2,3-c]pyrazole-5-carbonitrile derivatives were purified using recrystallization in ethanol.

After separation by the magnet, the zirconium magnetic nanocomposite was washed several times with a mixture of double-distilled water and ethanol and was reused after drying at room temperature.

6-amino-3-methyl-1,4-diphenyl-1,4-dihydropyran[2,3-c]pyrazole-5-carbonitrile (5a) FT-IR (KBr, cm^{-1}): 3402, 3284, 3181, 2203, 1675, 1660, 1529, 1461, 1317, 1240, 1101. $^1\text{H-NMR}$ (250 MHz, DMSO- d_6): δ (ppm) 7.64 (s, 1 H), 7.41–7.27 (m, 11 H), 4.73 (s, 1 H), 1.63 (s, 3 H). $^{13}\text{C-NMR}$ (75 MHz, DMSO- d_6): δ (ppm) 159.24, 144.86, 143.92, 143.61, 137.01, 128.92, 128.52, 128.07, 127.69, 127.12, 126.34, 119.96, 112.51, 97.96, 58.13, 11.73.

6-amino-4-(4-methoxyphenyl)-3-methyl-1-phenyl-1,4-dihydropyran[2,3-c]pyrazole-5-carbonitrile (5c) FT-IR (KBr, cm^{-1}): 3392, 3342, 3112, 2165, 1673, 1525, 1416, 1341, 12,120, 1114. $^1\text{H-NMR}$ (250 MHz, DMSO- d_6): δ (ppm) 7.69 (d, 2 H, $J = 8.4$ Hz), 7.42 (t, 2 H, $J = 8$ Hz), 7.35 (t, 1 H, $J = 7.8$ Hz), 7.19 (d, 4 H, $J = 8.4$ Hz), 6.95 (s, 2 H), 4.63 (s, 1 H), 3.62 (s, 3 H), 1.82 (s, 3 H). $^{13}\text{C-NMR}$ (75 MHz, DMSO- d_6): δ (ppm) 160.82, 145.62, 144.01, 143.25, 137.82, 129.07, 128.15, 128.52, 127.67, 127.35, 126.73, 119.03, 112.46, 97.34, 57.57, 12.01.

6-amino-4-(4-hydroxyphenyl)-3-methyl-1-phenyl-1,4-dihydropyran[2,3-c]pyrazole-5-carbonitrile (5i) FT-IR (KBr, cm^{-1}): 3381, 3313, 3157, 2189, 1670, 1538, 1402, 1321, 1249, 1157. $^1\text{H-NMR}$ (250 MHz, DMSO- d_6): δ (ppm) 9.28 (s, 1 H), 7.71 (d, 2 H, $J = 8.4$ Hz), 7.55–7.49 (t, 2 H, $J = 8.7$ Hz), 7.29–7.21 (t, 1 H, $J = 8.4$ Hz), 7.04 (s, 2 H), 7.11–7.14 (d, 2 H, $J = 7.5$ Hz), 6.71 (s, 2 H), 4.54 (s, 1 H), 1.77 (s, 3 H). $^{13}\text{C-NMR}$ (75 MHz, DMSO- d_6): δ (ppm); 160.11, 156.01, 144.98, 143.75, 143.08, 137.21, 133.62, 129.04, 128.66, 126.17, 120.49, 119.34, 114.99, 99.18, 58.61, 12.64.

2.4. Zirconium Magnetic Nanocomposite Antimicrobial Activity

To measure the MIC, MBC, and MFC, a concentration of 1–2048 mg/mL of zirconium magnetic nanocomposite and the drug were prepared. The Clinical and Laboratory Standards Institute (CLSI) guidelines (M07-A9, M26-A, M27-A2) were used for the zirconium magnetic nanocomposite antimicrobial activity. Based on the reported methods, relevant tests on the desired Gram-positive, Gram-negative species, and desired fungal species were performed [34–36].

3. Results

3.1. Results of Synthesis and Confirmation Structure of Zirconium Magnetic Nanocomposite

A new zirconium magnetic nanocomposite using Fe_3O_4 nanoparticles, pyridine-2,6 dicarboxylic acid, and zirconium (IV) chloride was synthesized under microwave irradiation. Various techniques and analyses, such as vibrating sample magnetometer curves (VSM, Magnetic Daghigh Danesh Pajoh Co, Iran, Kashan), X-ray diffraction patterns (XRD, Philips XPERT PRO, Netherlands, Eindhoven), scanning electron microscope images (SEM, Hitachi S-4800 FESEM, Japan, Tokyo) and transmission electron microscopy images (TEM, Philips EM 208S, Netherlands, Eindhoven), Fourier transform infrared spectroscopy (FT-IR, Thermo Scientific Nicolet-6700, Waltham, MA, USA), and Brunauer–Emmett–Teller N_2 adsorption/desorption isotherms (BET, Micromeritics, TriStar II 3020 analyser, Norcross, GA, USA), were used to identify and confirm the structure of the zirconium magnetic nanocomposite.

The magnetic saturation of the zirconium magnetic nanocomposite, as shown in the VSM curve in Figure 1, was 0.014 emu/g.

The magnetic property of the zirconium magnetic nanocomposite was compared with the magnetic property of the Fe_3O_4 nanoparticles. According to previous reports, the saturation value of the Fe_3O_4 nanoparticles was 0.055 emu/g [2]. The decrease in the magnetic saturation of the zirconium magnetic nanocomposite shows that the Fe_3O_4 nanoparticles were covered in groups.

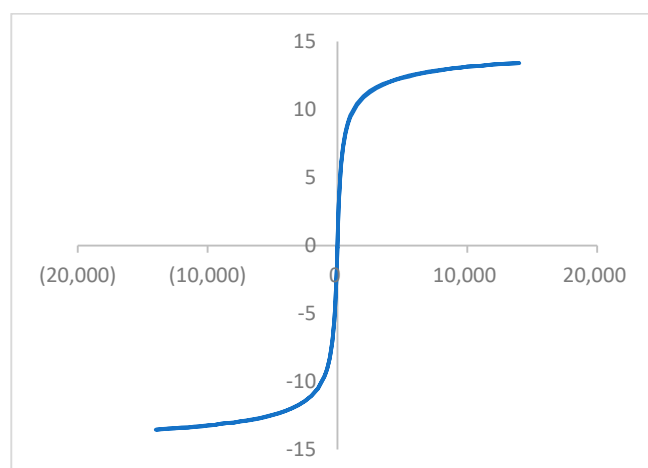


Figure 1. Magnetic saturation curve of zirconium magnetic nanocomposite.

The XRD pattern of the zirconium magnetic nanocomposite (Figure 2) confirmed the crystalline structure and the presence of Fe_3O_4 nanoparticles in the final product's structure [37].

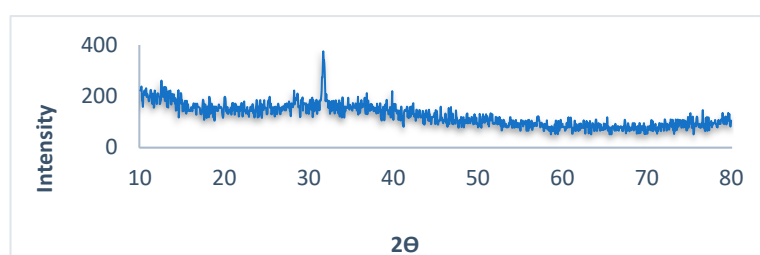


Figure 2. X-ray diffraction pattern of zirconium magnetic nanocomposite.

The SEM and TEM images of the zirconium magnetic nanocomposite (Figure 3) confirmed the uniformity of the structure and the morphology of the final product. In addition, the SEM and TEM images proved that the structure of the compound was in the nano-sized range.

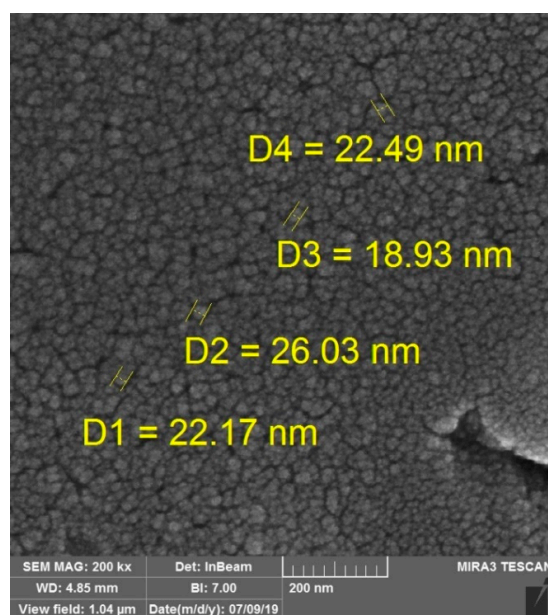


Figure 3. Cont.

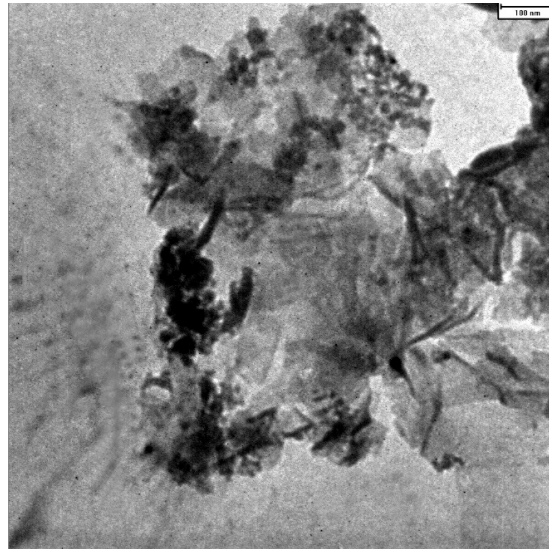


Figure 3. Scanning electron microscope and transmission electron microscopy images of zirconium magnetic nanocomposite.

The FT-IR spectrum of the zirconium magnetic nanocomposite, as shown in Figure 4, proved the desired absorptions of the final product's structure.

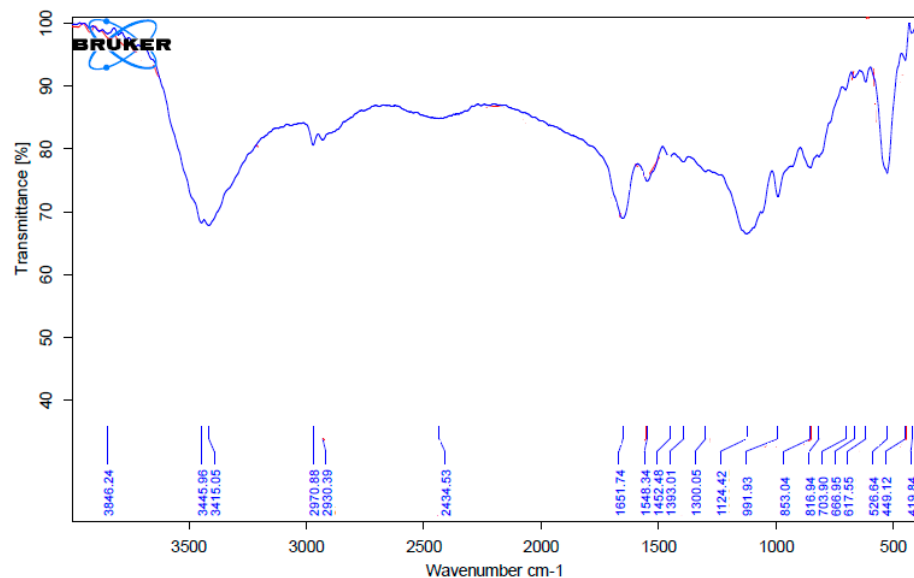


Figure 4. Fourier transform infrared spectroscopy of zirconium magnetic nanocomposite.

The Fe_3O_4 nanoparticles showed absorption in the region of 526 cm^{-1} . The peaks in areas 617 cm^{-1} and 667 cm^{-1} were related to Zr-O [38]. The peak observed in the region 1124 cm^{-1} corresponded to the C-O group. The C=C and C=O groups showed absorption in areas 1548 cm^{-1} and 1651 cm^{-1} , respectively. The absorption of the C-H group was observed in areas 2930 cm^{-1} and 2970 cm^{-1} . Finally, the absorption of the O-H group was observed in the 3400 cm^{-1} .

The N_2 adsorption/desorption isotherms of the zirconium magnetic nanocomposite were the fourth type of the classical isotherm series [39]. The specific surface area of the zirconium magnetic nanocomposite was about $1850\text{ m}^2/\text{g}$ (Figure 5).

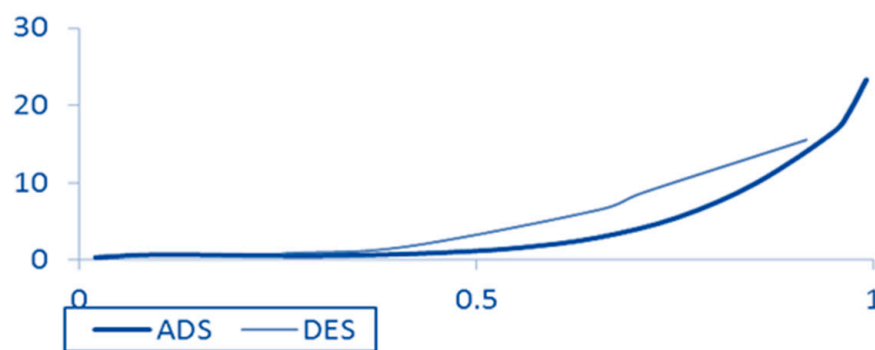


Figure 5. N_2 adsorption/desorption isotherms of zirconium magnetic nanocomposite.

As an overall finding, it can be stated that the synthetic compound had magnetic properties and could be easily separated in catalytic reactions. The desired elements and functional groups were observed in the structure of the synthesized compound. The synthesis method and microwave radiation caused uniform morphology and nano-sized particles. In addition, the synthesis method increased the specific surface area, which led to its use as an efficient catalyst and bioactive agent.

Based on the observations and spectral analysis, the following structure was suggested for the zirconium magnetic nanocomposite (Figure 6).

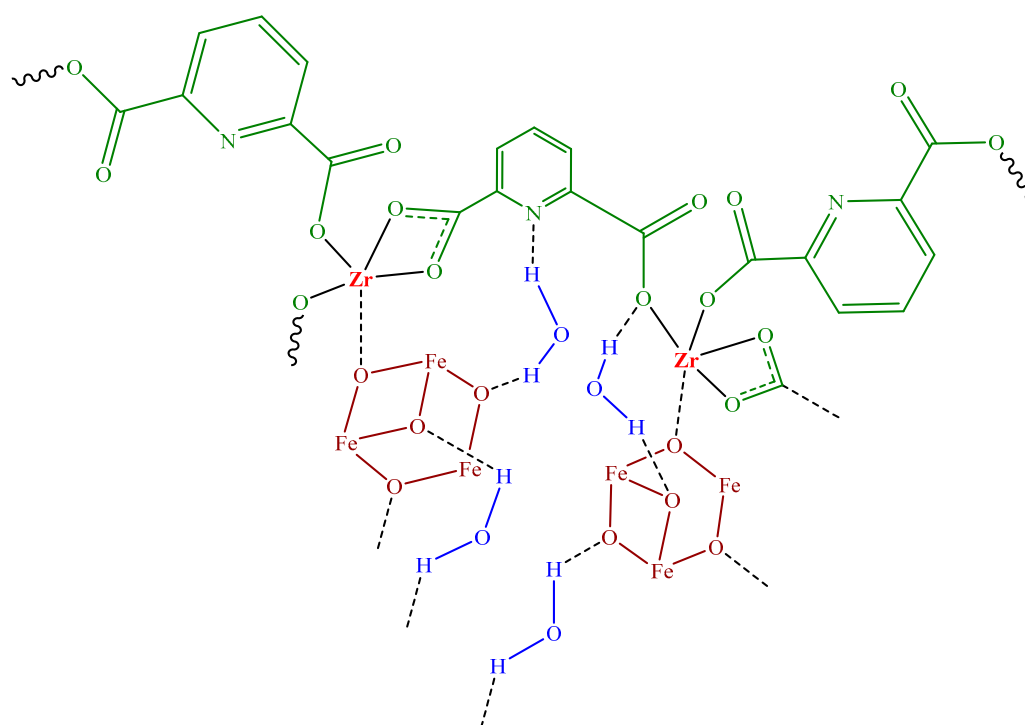
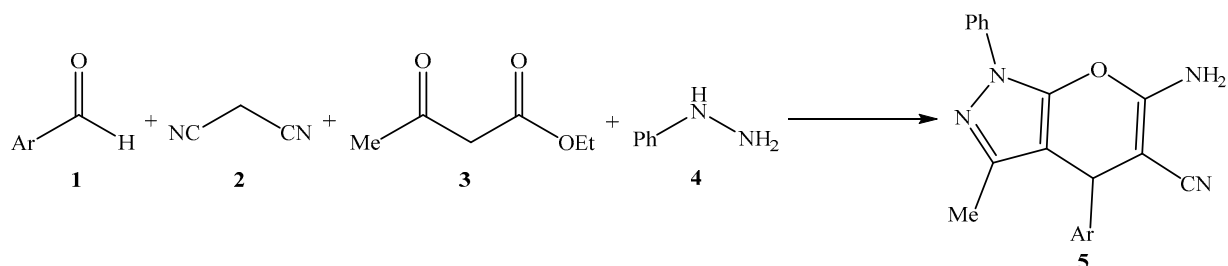


Figure 6. Suggested structure for zirconium magnetic nanocomposite.

3.2. Results of Four-Component Synthesis of Multi-Ring Compound Containing Pyrazole Using Zirconium Magnetic Nanocomposite

From the four-component reaction of the aromatic aldehyde derivatives, malononitrile, phenylhydrazine, and ethyl acetoacetate in the presence of the zirconium magnetic nanocomposite as a catalyst, 1,4-dihydropyrano[2,3-c]pyrazole-5-carbonitrile derivatives were synthesized (Scheme 1).



Scheme 1. Synthesis of 1,4-dihydropyrano[2,3-c]pyrazole-5-carbonitrile using aromatic aldehyde derivatives, malononitrile, phenylhydrazine, and ethyl acetoacetate.

To synthesize the derivatives, we first optimized the reaction conditions, such as the solvent, amount of catalyst, and temperature. Different solvents, such as EtOH, EtOH: H₂O (1:1), MeOH, and CH₃CN, were tested during optimization. Based on the obtained results, the highest efficiency was obtained using EtOH: H₂O.

To optimize the catalyst amount, the reactions in amounts of 1–5 mg were tested. Based on the obtained results, high efficiency was observed in using 4 mg as the catalyst. Finally, temperature optimization was performed, and the reaction at 50 °C had the highest yield. The optimization results are given in Table 1.

Table 1. Optimization of solvent, amount of catalyst, and temperature in the four-component synthesis of 1,4-dihydropyrano[2,3-c]pyrazole-5-carbonitrile.

Product	Solvent	Catalyst (mg)	Temperature (°C)	Time (min)	Yield (%)
5a	EtOH	2	50	25	80
5a	H ₂ O:EtOH (1:1)	2	50	25	87
5a	MeOH	2	50	45	34
5a	CH ₃ CN	2	50	60	21
5a	H ₂ O:EtOH (1:1)	1	50	30	75
5a	H ₂ O:EtOH (1:1)	3	50	25	90
5a	H ₂ O:EtOH (1:1)	4	50	20	95
5a	H ₂ O:EtOH (1:1)	5	50	20	93
5a	H ₂ O:EtOH (1:1)	4	r. t	45	71
5a	H ₂ O:EtOH (1:1)	4	40	30	89
5a	H ₂ O:EtOH (1:1)	4	60	20	94
5a	H ₂ O:EtOH (1:1)	4	80	25	86
5a	H ₂ O:EtOH (1:1)	4	reflux	25	83

The structures of the 16 derivatives of 1,4-dihydropyrano[2,3-c]pyrazole-5-carbonitrile (5a–o) synthesized in this study under optimal conditions are given in Table 2.

For synthesizing the 1,4-dihydropyrano[2,3-c]pyrazole-5-carbonitrile derivatives studied in this research using the zirconium magnetic nanocomposite as a catalyst, the Scheme 2 mechanism was proposed.

Table 2. 1,4-dihydropyrano[2,3-c]pyrazole-5-carbonitrile derivatives synthesized using zirconium magnetic nanocomposite as a catalyst.

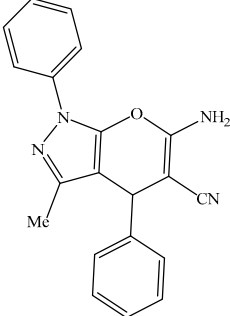
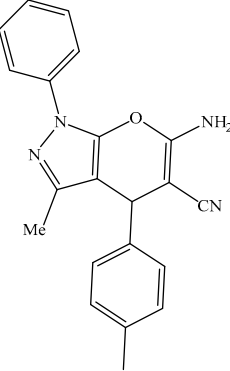
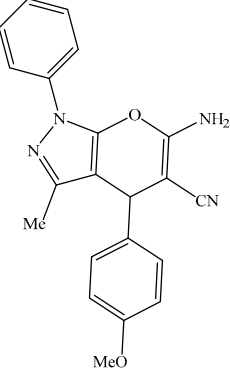
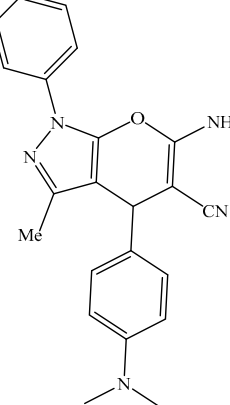
Product	Structure	Time (min)	Yield (%)	Mp (°C)	
				Found	Reported
5a		20	95	165–167	166–168 [40]
5b		45	90	170–172	173–175 [41]
5c		20	95	170–172	169–171 [42]
5d		25	87	220	219–222 [40]

Table 2. Cont.

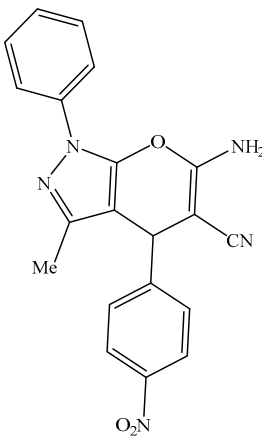
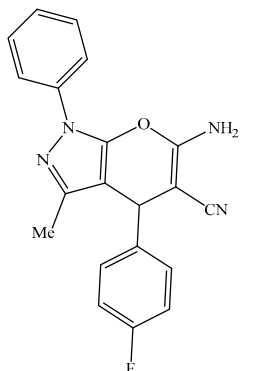
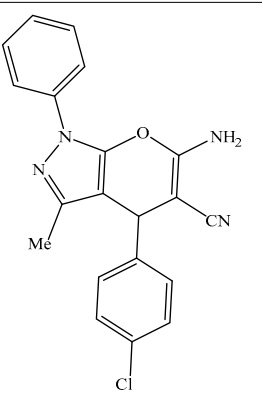
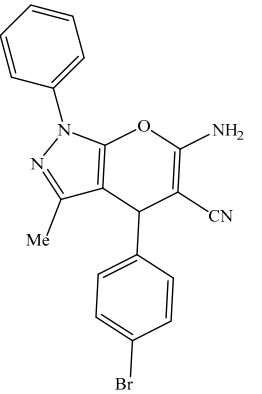
Product	Structure	Time (min)	Yield (%)	Mp (°C)	
				Found	Reported
5e		15	96	186–189	188–191 [40]
5f		20	91	168–170	170–172 [42]
5g		15	92	175–178	174–180 [40]
5h		20	92	176–178	175–180 [40]

Table 2. Cont.

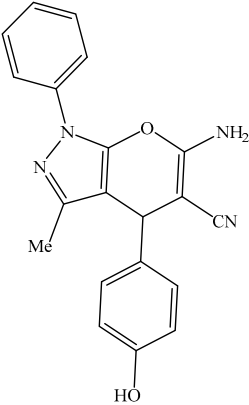
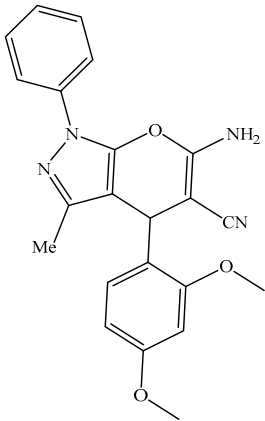
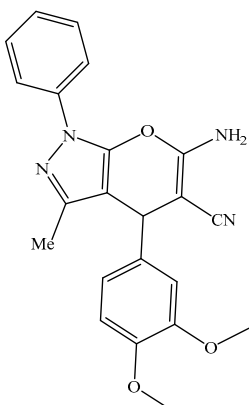
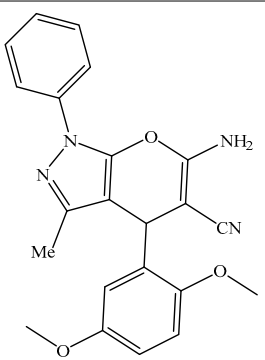
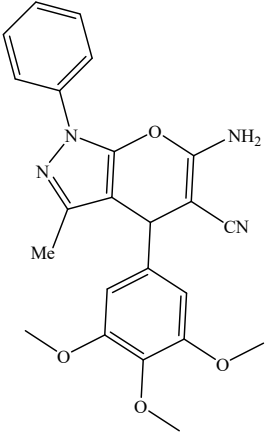
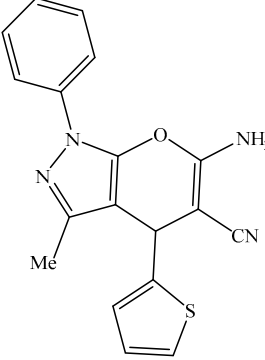
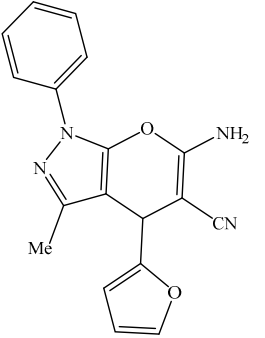
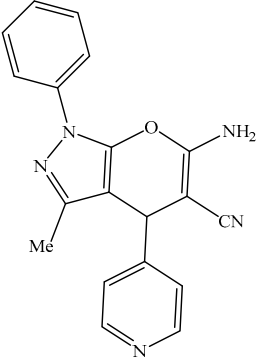
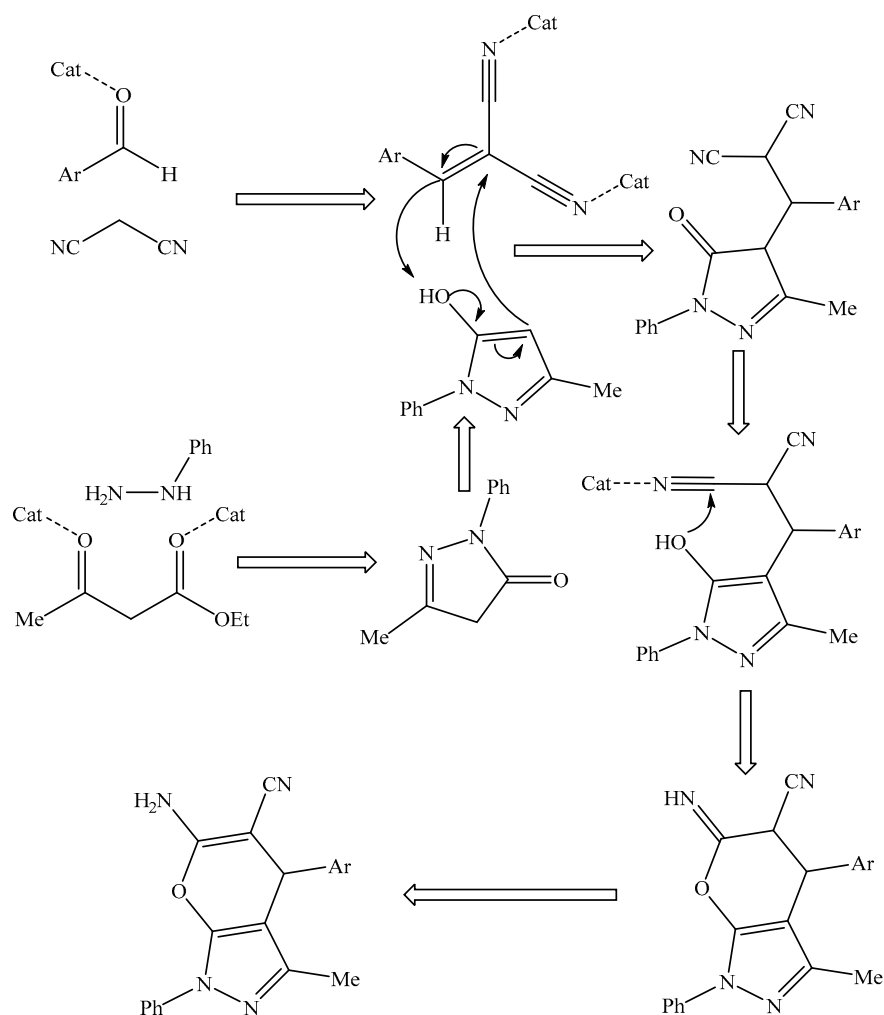
Product	Structure	Time (min)	Yield (%)	Mp (°C)	
				Found	Reported
5i		25	92	191–193	192–194 [43]
5j		20	90	175–176	176–178 [44]
5k		25	87	192–195	193–195 [45]
5l		30	85	207–210	209–211 [46]

Table 2. Cont.

Product	Structure	Time (min)	Yield (%)	Mp (°C)	
				Found	Reported
5m		20	89	196–198	194–196 [47]
5m		30	92	173–174	172–174 [48]
5n		60	90	226–229	225–228 [48]
5o		25	89	205–208	207–208 [49]



Scheme 2. Synthesis mechanism of 1,4-dihydropyrano[2,3-c]pyrazole-5-carbonitrile derivatives using zirconium magnetic nanocomposite.

Table 3 shows a comparison of the recently reported synthesis methods of 1,4-dihydropyrano[2,3-c]pyrazole-5-carbonitrile derivatives such as triazine-based functionalized HY zeolite [40], SBA-15/hydrotalcite/heteropoly acid (phosphotungstic acid) [50], tungstic acid immobilized on zirconium-L-aspartate amino acid metal-organic framework-grafted L-(+)-tartaric acid-stabilized magnetic Fe_3O_4 nanoparticles [51], yttrium iron garnet [52], triphenylphosphine [53], sugarcane bagasse ash-based silica-supported boric acid [54], and 1,3-dimethyl-2-oxo-1,3-bis(4-sulfobutyl) imidazolidine-1,3-dium hydrogen sulfate[DMDBSI] 2HSO_4 [55] as a catalyst.

As a result, the zirconium magnetic nanocomposite synthesized the desired product with better results, including higher efficiency, a shorter time, and a lower temperature.

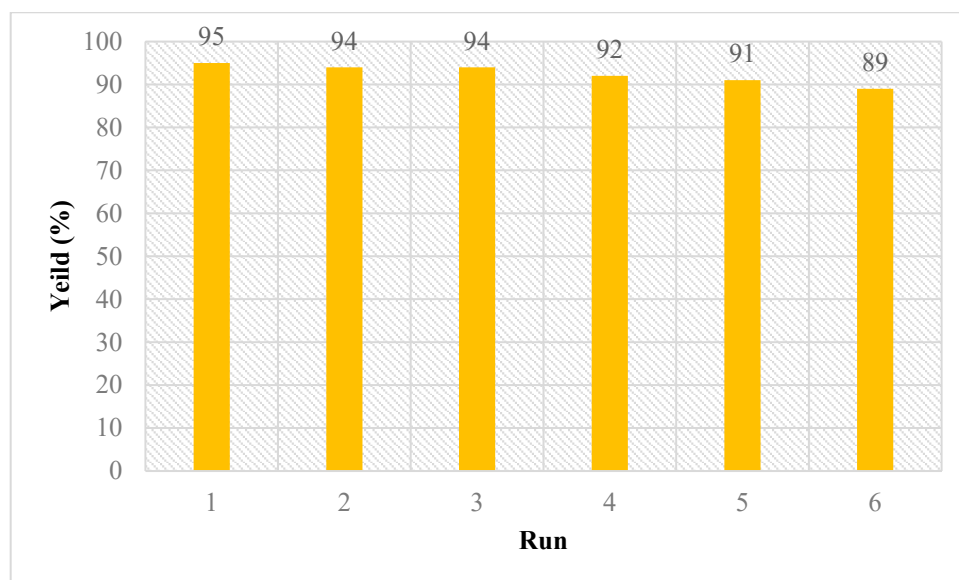
As mentioned earlier, the favorable conditions of the zirconium magnetic nanocomposite as a catalyst can be attributed to its high specific surface area.

Another essential advantage of the catalyst studied in this study was its recycling ability.

Figure 7 shows that the zirconium magnetic nanocomposite can be reused up to six times (for 5a), which does not significantly reduce the efficiency of the product.

Table 3. Comparison of synthesis methods of 1,4-dihydropyrano[2,3-c]pyrazole-5-carbonitrile with the method studied in this research.

Product	Condition	Time (min)	Temperature (°C)	Yield (%)
5a	triazine-based functionalized HY zeolite	50	80	95 [40]
5a	SBA-15/hydrotalcite/heteropoly acid (phosphotungstic acid)	20	reflux	93 [50]
5a	tungstic acid immobilized on zirconium-L-aspartate amino acid metal-organic framework-grafted L-(+)-tartaric acid-stabilized magnetic Fe ₃ O ₄ nanoparticles	45	60	92 [51]
5a	yttrium iron garnet	20	80	90 [52]
5a	triphenylphosphine	2h	reflux	87 [53]
5a	sugarcane bagasse ash-based silica-supported boric acid	35	75	86 [54]
5a	1,3-dimethyl-2-oxo-1,3-bis(4-sulfobutyl)imidazolidine-1,3-dium hydrogen sulfate[DMDBSI]2HSO ₄	15	60	85 [55]
5a	This work	20	50	95

**Figure 7.** The results of recycling the catalyst in the synthesis of 1,4-dihydropyrano[2,3-c]pyrazole-5-carbonitrile.

3.3. Results of Biological Activity of Zirconium Magnetic Nanocomposite

The high specific surface area of the zirconium magnetic nanocomposite synthesized in this study significantly affected the Gram-positive, Gram-negative, and fungal species. Zirconium magnetic nanocomposite's antimicrobial effects were tested based on the MIC (minimum inhibitory concentration), MBC (minimum bactericidal concentration), and MFC (minimum fungicidal concentration) parameters (Table 4).

The antibacterial effects of nanoparticles were examined on *Staphylococcus epidermidis* and *Bacillus cereus* (Gram-positive), *Klebsiella pneumonia* and *Shigella dysenteriae* (Gram-negative), and *Candida albicans* (fungi).

Furthermore, the antimicrobial effects of some commercial drugs (Cefazolin as an antibacterial drug and Terbinafine as an antifungal drug) on the studied species were tested to compare their effectiveness to the zirconium magnetic nanocomposite.

Table 4. Results of antibacterial and antifungal activity of zirconium magnetic nanocomposite compared to commercial drugs.

Zirconium Magnetic Nanocomposite and Drugs	Gram-Positive Bacteria Species				Gram-Negative Bacteria Species				Fungi Species	
	<i>Staphylococcusepidermidis</i>		<i>Bacillus cereus</i>		<i>Klebsiella pneumoniae</i>		<i>Shigelladysenteriae</i>		<i>Candida albicans</i>	
	MIC	MBC	MIC	MBC	MIC	MBC	MIC	MBC	MIC	MFC
Zirconium magnetic nanocomposite	8	16	64	128	32	64	128	256	64	128
Antibacterial drug	2	4	-	-	4	8	-	-	*	*
Antifungal drug	*	*	*	*	*	*	*	*	-	-

Antibacterial drug: Cefazolin; Antifungal drug: Terbinafine. Values are in $\mu\text{g}/\text{mL}$. * Not checked.

The results of the antimicrobial tests proved that the zirconium magnetic nanocomposite positively affected all studied Gram-positive, Gram-negative, and fungi species. The MBC value was 16 $\mu\text{g}/\text{mL}$ on *Staphylococcus epidermidis*, 128 $\mu\text{g}/\text{mL}$ on *Bacillus cereus*, 64 $\mu\text{g}/\text{mL}$ on *Klebsiella pneumoniae*, and 128 $\mu\text{g}/\text{mL}$ on *Shigella dysenteriae*, and the MFC value on *Candida albicans* was 128 $\mu\text{g}/\text{mL}$.

It is noteworthy that Cefazolin was ineffective on *Bacillus cereus* and *Shigella dysenteriae*, and Terbinafine was ineffective on *Candida albicans*. However, the zirconium magnetic nanocomposite had a positive effect.

As mentioned earlier, the unique properties of the zirconium magnetic nanocomposite can be attributed to its high specific surface area, which is the result of its synthesis method.

4. Conclusions

In the present study, a zirconium magnetic nanocomposite was synthesized using the microwave method. Analyses such as vibrating sample magnetometer curves, X-ray diffraction patterns, scanning electron microscope and transmission electron microscopy images, Fourier transform infrared spectroscopy, and Brunauer–Emmett–Teller N_2 adsorption/desorption isotherms to identify and confirm its structure were performed. The results of the analyses showed that the synthesis method caused uniform morphology and increased the specific surface area of the zirconium magnetic nanocomposite. The synthesized zirconium magnetic nanocomposite was used as a catalyst in the synthesis of 1,4-dihydropyrano[2,3-c]pyrazole-5-carbonitrile derivatives due to its unique properties, including its high specific surface area, which is essential for catalytic applications. The catalytic activity results compared to the previously reported methods for synthesizing 1,4-dihydropyrano[2,3-c]pyrazole-5-carbonitrile derivatives were significant. One of the other advantages of its use as a catalyst is its possible reuse without a noticeable decrease in efficiency. The high specific surface area of the zirconium magnetic nanocomposite resulted in biological activity, which was effective on Gram-positive, Gram-negative, and the studied fungal species. The noteworthy finding of the antibacterial activity was its higher effectiveness compared to the commercially used drugs.

Author Contributions: Study conception and design, R.D.L. and S.L.; data collection, M.A. and F.A.; analysis and interpretation of results, A.G.A. and M.K.; draft manuscript preparation, M.S. and S.K.H.; editing, R.D.L.; visualization, S.L.; supervision, D.A.M.; project administration, I.F. All authors have read and agreed to the published version of the manuscript.

Funding: This research received no external funding.

Data Availability Statement: The authors confirm that the data supporting the findings of this study are available within the article.

Acknowledgments: The authors extend their appreciation to the Deanship of Scientific Research at King Khalid University for funding this work through the extensive research group program under grant number (R.G.P.02/148/43).

Conflicts of Interest: The authors declare no conflict of interest.

References

1. Moonen, K.; Laureyn, I.; Stevens, C.V. Synthetic methods for azaheterocyclic phosphonates and their biological activity. *Chem. Rev.* **2004**, *104*, 6177–6216. [[CrossRef](#)] [[PubMed](#)]
2. Hosseinzadegan, S.; Hazeri, N.; Maghsoodlou, M.T.; Moghaddam-Manesh, M.; Shirzaei, M. Synthesis and evaluation of biological activity of novel chromeno [4,3-b] quinolin-6-one derivatives by SO₃ H-tryptamine supported on Fe₃O₄@ SiO₂@ CPS as recyclable and bioactive magnetic nanocatalyst. *J. Iran. Chem. Soc.* **2020**, *17*, 3271–3284. [[CrossRef](#)]
3. Etemadi, Y.; Shiri, A.; Eshghi, H.; Akbarzadeh, M.; Saadat, K.; Mozafari, S.; Beyzaei, H.; Moghaddam-Manesh, M. Synthesis, characterisation, and in vitro antibacterial evaluation of a new class of 2-substituted-4-methyl-7, 8-dihydro-5H-pyrimido [4, 5-d] thiazolo [3,2-a] pyrimidines. *J. Chem. Res.* **2016**, *40*, 600–603. [[CrossRef](#)]
4. Moghaddam-Manesh, M.; Hosseinzadegan, S. Introducing new method for the synthesis of polycyclic compounds containing [1,3] dithiine derivatives, with anticancer and antibacterial activities against common bacterial strains between aquatic and human. *J. Heterocycl. Chem.* **2021**, *58*, 2174–2180. [[CrossRef](#)]
5. Nath, R.; Pathania, S.; Grover, G.; Akhtar, M.J. Isatin containing heterocycles for different biological activities: Analysis of structure activity relationship. *J. Mol. Struct.* **2020**, *1222*, 128900. [[CrossRef](#)]
6. Moghaddam-Manesh, M.; Ghazanfari, D.; Sheikhsosseini, E.; Akhgar, M. Synthesis, Characterization and Antimicrobial Evaluation of Novel 6'-Amino-spiro [indeno [1,2-b] quinoxaline [1,3] dithiine]-5'-carbonitrile Derivatives. *Acta Chim. Slov.* **2020**, *67*, 276–282. [[CrossRef](#)]
7. Wang, X.; Wu, S.; Zhong, Y.; Wang, Y.; Pan, Y.; Tang, H. Electrochemically mediated decarboxylative acylation of N-nitrosoanilines with α -oxocarboxylic acids. *Chin. Chem. Lett.* **2022**, *34*, 107537. [[CrossRef](#)]
8. Ott, I. On the medicinal chemistry of gold complexes as anticancer drugs. *Coord. Chem. Rev.* **2009**, *253*, 1670–1681. [[CrossRef](#)]
9. Mihorianu, M.; Franz, M.H.; Jones, P.G.; Freytag, M.; Kelter, G.; Fiebig, H.H.; Tamm, M.; Neda, I. N-Heterocyclic carbenes derived from imidazo-[1,5-a] pyridines related to natural products: Synthesis, structure and potential biological activity of some corresponding gold (I) and silver (I) complexes. *Appl. Organomet. Chem.* **2016**, *30*, 581–589. [[CrossRef](#)]
10. Vollbrecht, A.; Neda, I.; Thönnessen, H.; Jones, P.G.; Schmutzler, R.; Harris, R.K.; Crowe, L.A. Synthesis, Structure, and Reactivity of Tetrakis (O, O-phosphorus)-Bridged Calix [4] resorcinols and Their Derivatives. *Chem. Ber.* **1997**, *130*, 1715–1720. [[CrossRef](#)]
11. Plinta, H.-J.; Neda, I.; Schmutzler, R. 1,3-Dimethyl-1, 3-diaza-2-R-5, 6-benzo-2 λ 3-phosphorinan-4-one (R = F, Me₂N, 2-Methylpiperidino, MeC (: 0) NH-) als Liganden in Übergangsmetallkomplexen; Synthese und Struktur von Dichloro-Platin (II)-und Tetracarbonyl-Metall (O)-Koordinationsverbindungen (Metall = Cr, Mo und W)/1,3-Dimethyl-1, 3-diaza-2-R-5, 6-benzo-2 λ 3-phosphorinan-4-ones (R = F, Me₂N, 2-Methylpiperidino, MeC (: 0) NH-) as Ligands in Transition-Metal Complexes; Synthesis and Structure of Dichloro-Platinum (II)-and Tetracarbonyl-Metal (0) Coordination Compounds (Metal = Cr, Mo and W). *Z. Nat. B* **1994**, *49*, 100–110.
12. Marichev, K.O.; Patil, S.A.; Patil, S.A.; Heras Martinez, H.M.; Bugarin, A. N-heterocyclic carbene metal complexes as therapeutic agents: A patent review. *Expert Opin. Ther. Pat.* **2022**, *32*, 47–61. [[CrossRef](#)]
13. Kumar, V.; Kaur, K.; Gupta, G.K.; Sharma, A.K. Pyrazole containing natural products: Synthetic preview and biological significance. *Eur. J. Med. Chem.* **2013**, *69*, 735–753. [[CrossRef](#)] [[PubMed](#)]
14. Kumar, H.; Saini, D.; Jain, S.; Jain, N. Pyrazole scaffold: A remarkable tool in the development of anticancer agents. *Eur. J. Med. Chem.* **2013**, *70*, 248–258. [[CrossRef](#)]
15. Reddy, T.S.; Kulhari, H.; Reddy, V.G.; Bansal, V.; Kamal, A.; RaviShukla. Design, synthesis and biological evaluation of 1,3-diphenyl-1H-pyrazole derivatives containing benzimidazole skeleton as potential anticancer and apoptosis inducing agents. *Eur. J. Med. Chem.* **2015**, *101*, 790–805. [[CrossRef](#)] [[PubMed](#)]
16. Abdellatif, K.R.; Fadaly, W.A.; Kamel, G.M.; Elshaiyer, Y.A.; El-Magd, M.A. Design, synthesis, modeling studies and biological evaluation of thiazolidine derivatives containing pyrazole core as potential anti-diabetic PPAR- γ agonists and anti-inflammatory COX-2 selective inhibitors. *Bioorg. Chem.* **2019**, *82*, 86–99. [[CrossRef](#)]
17. Bakthavatchala Reddy, N.; Zyryanov, G.V.; Mallikarjuna Reddy, G.; Balakrishna, A.; Padmaja, A.; Padmavathi, V.; Suresh Reddy, C.; Garcia, J.R.; Sravya, G. Design and synthesis of some new benzimidazole containing pyrazoles and pyrazolyl thiazoles as potential antimicrobial agents. *J. Heterocycl. Chem.* **2019**, *56*, 589–596. [[CrossRef](#)]
18. Verma, R.; Verma, S.K.; Rakesh, K.P.; Girish, Y.R.; Ashrafizadeh, M.; Kumar, K.S.S.; Rangappa, K.S. Pyrazole-based analogs as potential antibacterial agents against methicillin-resistance staphylococcus aureus (MRSA) and its SAR elucidation. *Eur. J. Med. Chem.* **2021**, *212*, 113134. [[CrossRef](#)]
19. Kumari, S.; Paliwal, S.K.; Chauhan, R. An improved protocol for the synthesis of chalcones containing pyrazole with potential antimicrobial and antioxidant activity. *Curr. Bioact. Compd.* **2018**, *14*, 39–47. [[CrossRef](#)]
20. Kar, S.; Sanderson, H.; Roy, K.; Benfenati, E.; Leszczynski, J. Green Chemistry in the Synthesis of Pharmaceuticals. *Chem. Rev.* **2021**, *122*, 3637–3710. [[CrossRef](#)]
21. Ou, C.-H.; Pan, Y.-M.; Tang, H.-T. Electrochemically promoted N-heterocyclic carbene polymer-catalyzed cycloaddition of aldehyde with isocyanide acetate. *Sci. China Chem.* **2022**, *65*, 1873–1878. [[CrossRef](#)]
22. Arlan, F.M.; Marjani, A.P.; Javahershenas, R.; Khalafy, J. Recent developments in the synthesis of polysubstituted pyridines via multi-component reactions using nanocatalysts. *New J. Chem.* **2021**, *45*, 12328–12345. [[CrossRef](#)]

23. Hosseinzadegan, S.; Hazeri, N.; Maghsoodlou, M.T. Synthesis and evaluation of antimicrobial and antioxidant activity of novel 7-Aryl-6H, 7H-benzo [f] chromeno [4, 3-b] chromen-6-one by MgO nanoparticle as green catalyst. *J. Heterocycl. Chem.* **2020**, *57*, 621–626. [[CrossRef](#)]
24. Kumar, P.P.; Bhatlu, M.L.D.; Sukanya, K.; Karthikeyan, S.; Jayan, N. Synthesis of magnesium oxide nanoparticle by eco friendly method (green synthesis)—A review. *Mater. Today Proc.* **2021**, *37*, 3028–3030. [[CrossRef](#)]
25. Ghafari, H. Transition metal-free oxidation of benzylic alcohols to carbonyl compounds by hydrogen peroxide in the presence of acidic silica gel. *Curr. Chem. Lett.* **2015**, *4*, 27–32. [[CrossRef](#)]
26. Aghaei-Hashjin, M.; Yahyazadeh, A.; Abbaspour-Gilandeh, E. Mo@ GAA-Fe₃O₄ MNPs: A highly efficient and environmentally friendly heterogeneous magnetic nanocatalyst for the synthesis of polyhydroquinoline derivatives. *RSC Adv.* **2021**, *11*, 10497–10511. [[CrossRef](#)]
27. Feng, X.; Xia, L.; Jiang, Z.; Tian, M.; Zhang, S.; He, C. Dramatically promoted toluene destruction over Mn@ Na-Al₂O₃@ Al monolithic catalysts by Ce incorporation: Oxygen vacancy construction and reaction mechanism. *Fuel* **2022**, *326*, 125051. [[CrossRef](#)]
28. Yao, X.; Bai, C.; Chen, J.; Li, Y. Efficient and selective green oxidation of alcohols by MOF-derived magnetic nanoparticles as a recoverable catalyst. *RSC Adv.* **2016**, *6*, 26921–26928. [[CrossRef](#)]
29. Yan, J.; Liu, T.; Liu, X.; Yan, Y.; Huang, Y. Metal-organic framework-based materials for flexible supercapacitor application. *Coord. Chem. Rev.* **2022**, *452*, 214300. [[CrossRef](#)]
30. Dourandish, Z.; Tajik, S.; Beitollahi, H.; Jahani, P.M.; Nejad, F.G.; Sheikhshoae, I.; Di Bartolomeo, A. A Comprehensive Review of Metal–Organic Framework: Synthesis, Characterization, and Investigation of Their Application in Electrochemical Biosensors for Biomedical Analysis. *Sensors* **2022**, *22*, 2238. [[CrossRef](#)]
31. Liu, W.; Huang, F.; Liao, Y.; Zhang, J.; Ren, G.; Zhuang, Z.; Zhen, J.; Lin, Z.; Wang, C. Treatment of CrVI-Containing Mg(OH)₂ Nanowaste. *Angew. Chem.* **2008**, *120*, 5701–5704. [[CrossRef](#)]
32. Martín, N.; Dusselier, M.; De Vos, D.E.; Cirujano, F.G. Metal-Organic framework derived metal oxide clusters in porous aluminosilicates: A catalyst design for the synthesis of bioactive aza-heterocycles. *ACS Catal.* **2018**, *9*, 44–48. [[CrossRef](#)]
33. Niknam, E.; Panahi, F.; Daneshgar, F.; Bahrami, F.; Khalafi-Nezhad, A. Metal–organic framework MIL-101 (Cr) as an efficient heterogeneous catalyst for clean synthesis of benzoazoles. *ACS Omega* **2018**, *3*, 17135–17144. [[CrossRef](#)] [[PubMed](#)]
34. Abdieva, G.A.; Patra, I.; Al-Qargholi, B.; Shahryari, T.; Chauhan, N.P.S.; Moghaddam-Manesh, M. An Efficient Ultrasound-Assisted Synthesis of Cu/Zn Hybrid MOF Nanostructures With High Microbial Strain Performance. *Front. Bioeng. Biotechnol.* **2022**, *10*, 861580. [[CrossRef](#)] [[PubMed](#)]
35. Zeraati, M.; Moghaddam-Manesh, M.; Khodamoradi, S.; Hosseinzadegan, S.; Golpayegani, A.; Chauhan, N.P.S.; Sargazi, G. Ultrasonic assisted reverse micelle synthesis of a novel Zn-metal organic framework as an efficient candidate for antimicrobial activities. *J. Mol. Struct.* **2022**, *1247*, 131315. [[CrossRef](#)]
36. Moghaddam-Manesh, M.; Ghazanfari, D.; Sheikhsosseini, E.; Akhgar, M. MgO-Nanoparticle-Catalyzed Synthesis and Evaluation of Antimicrobial and Antioxidant Activity of New Multi-Ring Compounds Containing Spiro [indoline-3, 4'-[1, 3] dithiine]. *ChemistrySelect* **2019**, *4*, 9247–9251. [[CrossRef](#)]
37. Shiri, L.; Narimani, H.; Kazemi, M. Synthesis and characterization of sulfamic acid supported on Fe₃O₄ nanoparticles: A green, versatile and magnetically separable acidic catalyst for oxidation reactions and Knoevenagel condensation. *Appl. Organomet. Chem.* **2018**, *32*, e3927. [[CrossRef](#)]
38. Mallakpour, S.; Shafiee, E. The synthesis of poly(vinyl chloride) nanocomposite films containing ZrO(2) nanoparticles modified with vitamin B(1) with the aim of improving the mechanical, thermal and optical properties. *Des. Monomers Polym.* **2017**, *20*, 378–388. [[CrossRef](#)]
39. Mirhosseini, H.; Shamspur, T.; Mostafavi, A.; Sargazi, G. A novel ultrasonic reverse micelle-assisted electrospun efficient route for Eu-MOF and Eu-MOF/CA composite nanofibers: A high performance photocatalytic treatment for removal of BG pollutant. *Environ. Sci. Pollut. Res.* **2021**, *28*, 4317–4328. [[CrossRef](#)]
40. Alimohammadi, E.; Kaveh, K.; Ali, Z.M. Preparation of triazine-based functionalized HY zeolite and its application in the green synthesis of tetrahydrobenzo [b] pyran and 1, 4-dihydropyrano [2, 3-c] pyrazole derivatives as a novel mesoporous recyclable nanocatalyst. *J. Iran. Chem. Soc.* **2022**, *19*, 4721–4734. [[CrossRef](#)]
41. Eftekhari far, B.; Nasr-Esfahani, M. Synthesis, characterization and application of Fe₃O₄@ SiO₂@ CPTMO@ DEA-SO₃H nanoparticles supported on bentonite nanoclay as a magnetic catalyst for the synthesis of 1, 4-dihydropyrano [2, 3-c] pyrazoles. *Appl. Organomet. Chem.* **2020**, *34*, e5406. [[CrossRef](#)]
42. Solgi, M.; Khazaei, A.; Akbarpour, T. Synthesis of magnetic nanoparticles Fe₃O₄@ CQD@ Si (OEt)(CH₂)₃@ melamine@ TC@ Ni (NO₃) with application in the synthesis of 2-amino-3-cyanopyridine and pyrano [2, 3-c] pyrazole derivatives. *Res. Chem. Intermed.* **2022**, *48*, 2443–2468. [[CrossRef](#)]
43. Heravi, M.M.; Malakooti, R.; Kafshdarzadeh, K.; Amiri, Z.; Zadsirjan, V.; Atashin, H. Supported palladium oxide nanoparticles in Al-SBA-15 as an efficient and reusable catalyst for the synthesis of pyranopyrazole and benzylpyrazolyl coumarin derivatives via multi-component reactions. *Res. Chem. Intermed.* **2022**, *48*, 203–234. [[CrossRef](#)]
44. Balaskar, R.S.; Gavade, S.N.; Mane, M.S.; Shingate, B.B.; Shingare, M.S.; Mane, D.V. Greener approach towards the facile synthesis of 1, 4-dihydropyrano [2, 3-c] pyrazol-5-yl cyanide derivatives at room temperature. *Chin. Chem. Lett.* **2010**, *21*, 1175–1179. [[CrossRef](#)]

45. Shi, D.; Mou, J.; Zhuang, Q.; Niu, L.; Wu, N.; Wang, X. Three-component one-pot synthesis of 1, 4-dihydropyrano [2, 3-c] pyrazole derivatives in aqueous media. *Synth. Commun.* **2004**, *34*, 4557–4563. [[CrossRef](#)]
46. Irani, S.; Maghsoodlou, M.T.; Hadavi, M.S.; Hazeri, N.; Lashkari, M. Ag/TiO₂ Nano Thin Films Catalyzed Efficient Synthesis of 6-Amino-4-Aryl-3-Methyl-1, 4-Dihydropyrano [2, 3-C] Pyrazole-5-Carbonitriles at Green Conditions. *Orient. J. Chem.* **2017**, *33*, 814. [[CrossRef](#)]
47. Iravani, N.; Keshavarz, M.; Kish, H.A.S.; Parandvar, R. Tin sulfide nanoparticles supported on activated carbon as an efficient and reusable Lewis acid catalyst for three-component one-pot synthesis of 4H-pyrano [2, 3-c] pyrazole derivatives. *Chin. J. Catal.* **2015**, *36*, 626–633. [[CrossRef](#)]
48. Tahmassebi, D.; Blevins, J.E.; Gerardot, S.S. Zn (L-proline) 2 as an efficient and reusable catalyst for the multi-component synthesis of pyran-annulated heterocyclic compounds. *Appl. Organomet. Chem.* **2019**, *33*, e4807. [[CrossRef](#)]
49. Zolfigol, M.A.; Ayazi-Nasrabadi, R.; Baghery, S.; Khakyzadeh, V.; Azizian, S. Applications of a novel nano magnetic catalyst in the synthesis of 1, 8-dioxo-octahydroxanthene and dihydropyrano [2, 3-c] pyrazole derivatives. *J. Mol. Catal. A Chem.* **2016**, *418*, 54–67. [[CrossRef](#)]
50. Sadjadi, S.; Heravi, M.M.; Zadsirjan, V.; Farzaneh, V. A ternary hybrid system based on combination of mesoporous silica, heteropolyacid and double-layered clay: An efficient catalyst for the synthesis of 2, 4-dihydro-3H-pyrazol-3-ones and pyranopyrazoles in aqueous medium: Studying the effect of the synthetic procedure on the catalytic activity. *Res. Chem. Intermed.* **2018**, *44*, 6765–6785.
51. Khademi, S.; Zahmatkesh, S.; Aghili, A.; Badri, R. Tungstic acid (H₄WO₅) immobilized on magnetic-based zirconium amino acid metal-organic framework: An efficient heterogeneous Brønsted acid catalyst for 1-(4-phenyl)-2, 4-dihydropyrano [2, 3c] pyrazole derivatives preparation. *Appl. Organomet. Chem.* **2021**, *35*, e6192. [[CrossRef](#)]
52. Sedighinia, E.; Badri, R.; Kiasat, A. Application of yttrium iron garnet as a powerful and recyclable nanocatalyst for one-pot synthesis of pyrano [2, 3-c] pyrazole derivatives under solvent-free conditions. *Russ. J. Org. Chem.* **2019**, *55*, 1755–1763. [[CrossRef](#)]
53. Amine Khodja, I.; Fisli, A.; Lebour, O.; Boulcina, R.; Boumoud, B.; Debache, A. Four-component synthesis of pyrano [2, 3-c] pyrazoles catalyzed by triphenylphosphine in aqueous medium. *Lett. Org. Chem.* **2016**, *13*, 85–91. [[CrossRef](#)]
54. Pandey, A.; Kumar, A.; Shrivastava, S. Sugarcane Bagasse Ash-Based Silica-Supported Boric Acid (SBA-SiO₂-H₃BO₃): A Versatile and Reusable Catalyst for the Synthesis of 1, 4Dihydropyrano [2, 3c] pyrazole Derivatives. *Russ. J. Org. Chem.* **2021**, *57*, 653–660. [[CrossRef](#)]
55. Zakeri, M.; Nasef, M.M.; Kargaran, T.; Ahmad, A.; Abouzari-Lotf, E.; Asadi, J. Synthesis of pyrano [2, 3-c] pyrazoles by ionic liquids under green and eco-safe conditions. *Res. Chem. Intermed.* **2017**, *43*, 717–728. [[CrossRef](#)]